Article

Tuning the Surface Plasmon Resonance of Gold Dumbbell Nanorods

Puskar Chapagain,* Grégory Guisbiers, Matthew Kusper, Luke D. Geoffrion, Mourad Benamara, Alexander Golden, Abdel Bachri, and Lionel Hewavitharana

Read Online

ACCESS | Metrics & More | Article Recommendations | Supporting Information

ABSTRACT: Gold has always fascinated humans, occupying an important functional and symbolic role in civilization. In earlier times, gold was predominantly used in jewelry; today, this noble metal's surface properties are taken advantage of in catalysis and plasmonics. In this article, the plasmon resonance of gold dumbbell nanorods is investigated. This unusual morphology was obtained by a seed-mediated growth method. The concentration of chemical precursors such as cetyltrimethylammonium bromide and silver nitrate plays a significant role in controlling the shape of the nanorods. Indeed, the aspect ratio of dumbbell nanostructures was varied from 2.6 to 4. UV−visible absorption spectra revealed a shift of the longitudinal surface plasmon resonance peak from 669 to 789 nm. Having the plasmon resonance in the near infrared region helps to use those nanostructures as photothermal agents.
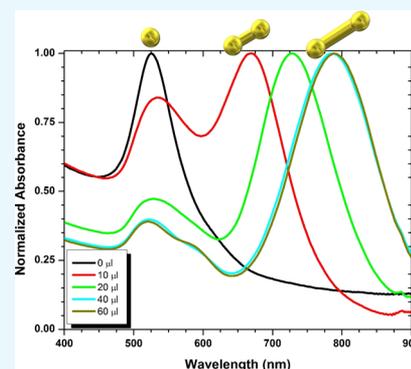
1. INTRODUCTION

Noble metals such as gold have always played a significant role in our civilization.[1,2] Nowadays, gold's continued use can be found in microelectronics, biomedical imaging, metallurgy, and catalysis. The size and shape of nanostructures affect many of the chemical, optical, and electronic properties.[3−5] Moreover, it has been reported that nanostructures could serve as the building blocks to form more complex structures.[6,7] Because of the morphological dependence of nanoparticle properties, controlling the shape and size of such particles has been the focus of many research studies. Gold nanorods (GNRs), in particular, are exciting materials because of their plasmonic properties for photonic applications. Researchers have used various methods including the electrochemical deposition on hard templates,[8] electrochemical synthesis in solutions,[3,9] photochemical synthesis,[9] and wet chemical synthesis[10] to produce GNRs.

Longitudinal gold nanostructures are very interesting as their optoelectronic properties can be tuned from visible to the NIR region by controlling the aspect ratio, crystallinity, and their environment within the colloidal solution. For example, modification of structure's endcap of nanorods could bring the shift up to 100 nm for longitudinal surface plasmon resonance (LSPR).[11] Chemicals adsorbed onto the surface of nanorods exhibit surface-enhanced Raman scattering (SERS) due to the interaction of gold surface plasmons with the electronic states of molecules via photoexcitation.[10,12] This is because longitudinal gold nanoparticles such as dumbbell-shaped, dog-bone-shaped, and phi-shaped are considered an important class of materials. These elongated particles exhibit potential use in various applications in optical sensors, biomedicine, imaging, and optoelectronic devices.[13] In this

paper, a seed-mediated method (SMG) to synthesize gold nanodumbbells (GNDs) is presented, allowing the surface plasmon properties to be tuned. Most previous work on gold nanostructures concentrated on the synthesis and characterization of uniform nanorods and dog-bone-shaped particles with little attention on GNDs. Even in previously published works, GNDs are treated as transition particles from GNRs to gold nanospheres.[14]

As mentioned previously, there is a minimal amount of work focusing purely on GNDs, but the synthesis of GNDs begins with the formation of GNRs, which have been adequately investigated. The work presented in this paper focused on the effect of cetyltrimethylammonium bromide (CTAB) and silver nitrate ($AgNO_3$) on the formation of GNDs, which is a common way to use a mixture of two surfactants during the synthesis process to control their shape, size, and optical properties.[15] We have characterized the GNDs and established the variation of aspect ratio with CTAB and $AgNO_3$. The results could determine the required amount of CTAB and $AgNO_3$ to produce GNDs with the desired aspect ratio. The following sections present their chemical synthesis, characterization, and results.
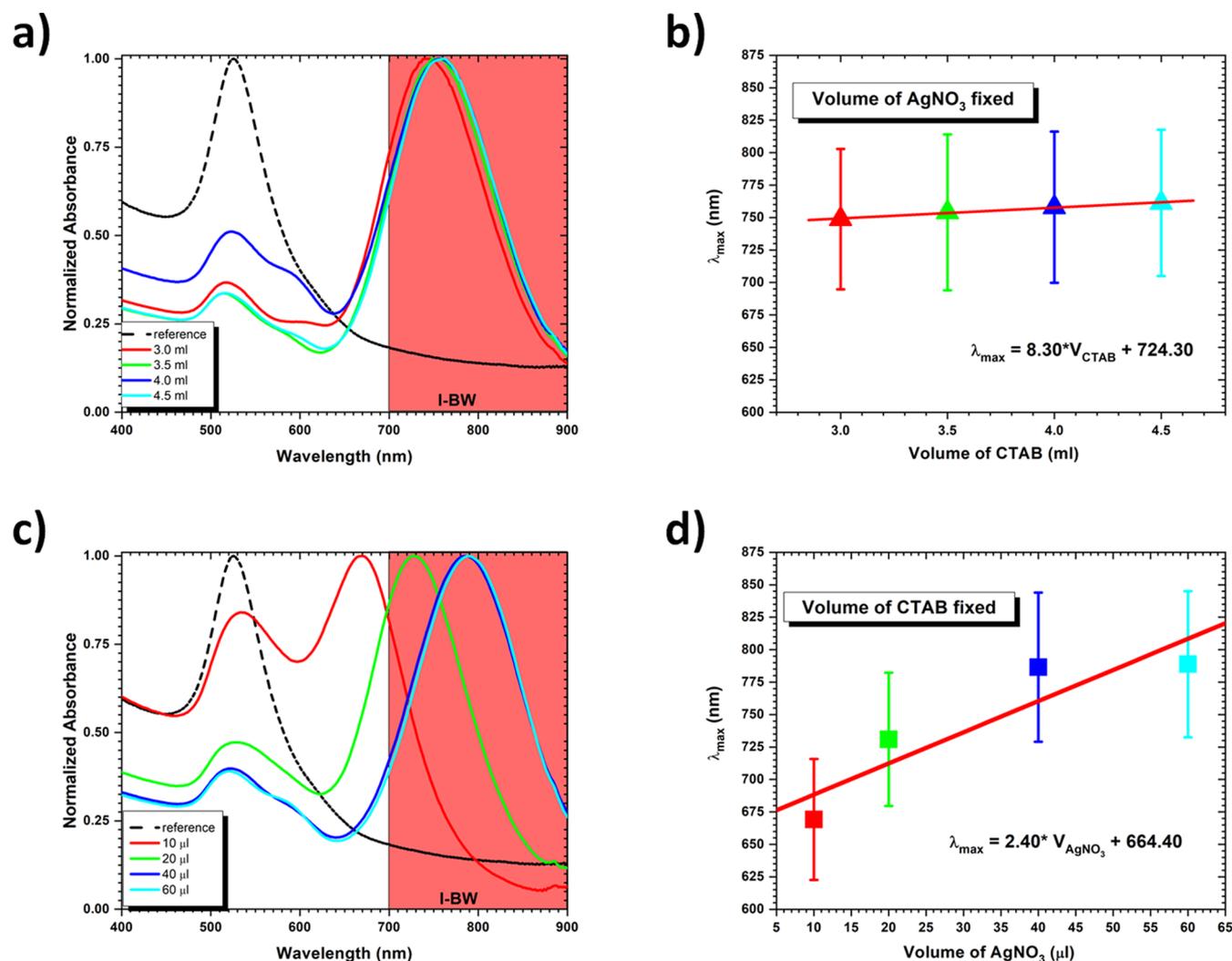
Figure 1. Effect of the precursors on the dumbbell growth. (a) Normalized absorption spectra of GNRs at different concentrations of CTAB (the volume concentration of CTAB at 3.0, 3.5, 4.0, and 4.5 mL corresponds to the molar concentration of 0.08902, 0.09044, 0.0915, and 0.0924 M, respectively). (b) LSPR peak position as a function of CTAB. (c) Normalized UV−vis absorption spectra with the variation of AgNO$_3$ (the volume concentration of AgNO$_3$ at 10, 20, 40, and 60 μL corresponds to the molar concentration of 1.9×10^{-5}, 3.7×10^{-5}, 7.4×10^{-5}, and 1.1×10^{-4} M, respectively). (d) Shift of the LSPR peak to longer wavelengths as an effect of AgNO$_3$. The dashed line in (a,c) corresponds to the gold plasmon resonance at 525 nm. The first biological window (I-BW) is also marked for reference.

2. RESULTS

2.1. Effect of CTAB on the Formation of Au-NRs.
Figure 1a shows the normalized UV−visible spectra obtained by the variation of the concentration of CTAB. Each spectrum reveals two significant peaks at approximately ∼525 and ∼750 nm corresponding to the transverse surface plasmon and the LSPR with a shoulder around 600 nm by fitting the normalized spectra with three Gaussian peaks. Figure 1b shows a very slim range of increase of LSPR with the concentration of CTAB, suggesting that CTAB could be responsible for slight elongation of the nanorods. However, the growth of the nanorods along the longitudinal direction occurs within a narrow range of CTAB.

2.2. Effect of AgNO$_3$ on the Formation of Au-NRs.
The effect of AgNO$_3$ variation on the formation of nanorods is shown in Figure 1c, demonstrating the significant role AgNO$_3$ plays in the formation of nanorods. In the absence of silver ions, only the peak corresponding to the transversal mode is observed at ∼520 nm. As the concentration of AgNO$_3$ increases, the peak corresponding to the longitudinal axis

∼720 nm starts to emerge. Moreover, as the concentration of AgNO$_3$ increases, the LSPR peak shifts toward a longer wavelength with the appearance of a shoulder of the peak for transverse surface plasmon resonance (TSPR), suggesting that the particles formed are different from the uniform nanorods. Figure 1d shows that the LSPR peak position varies with the linear function of the concentration of AgNO$_3$. This observation suggests that silver ions are the major contributors to the growth of the nanorods.

2.3. Effect of Concentration of Precursors on the Aspect Ratio.
Figure 2a,b shows the variation of aspect ratio with the volume of CTAB and AgNO$_3$. It appears that the aspect ratio of the rods varies linearly with the CTAB concentration, as well as with the concentration of AgNO$_3$, suggesting that the maximum possible aspect ratio of the current synthesis method is 4.

2.4. Separation of Rods from Spheres.
In order to separate anisotropic particles from isotropic particles within the colloidal solution, a two-step centrifugation process was used as prescribed in ref 16:
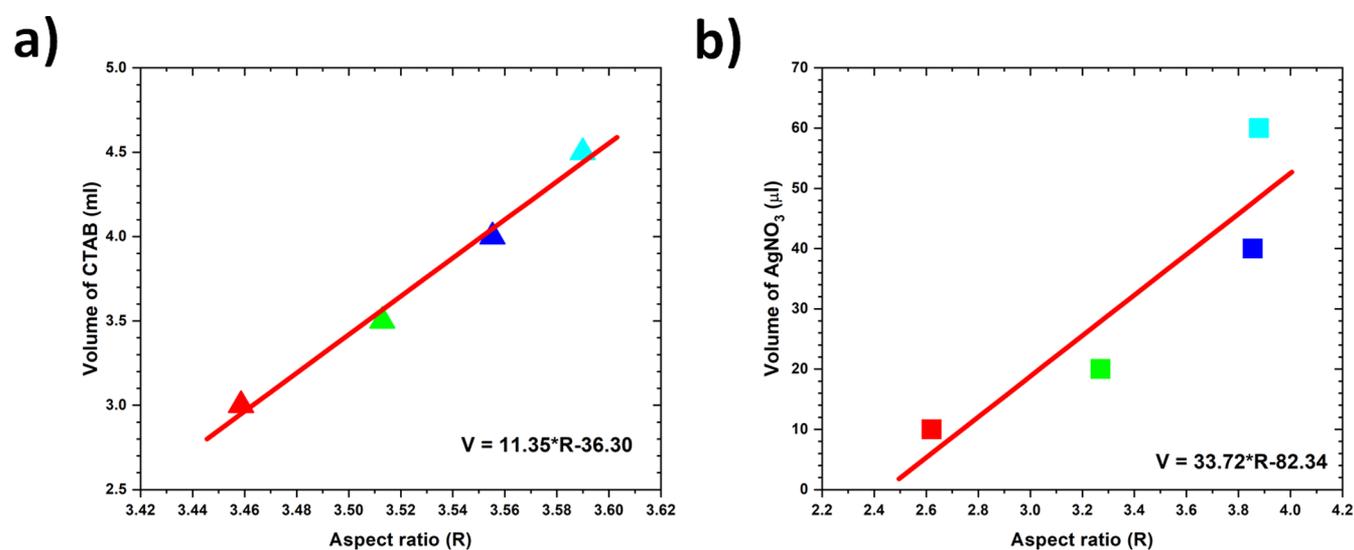
Figure 2. Effect of concentration of (a) CTAB and (b) AgNO$_3$ on the aspect ratio of dumbbell-shaped particles. Aspect ratio increases linearly with CTAB and AgNO$_3$.
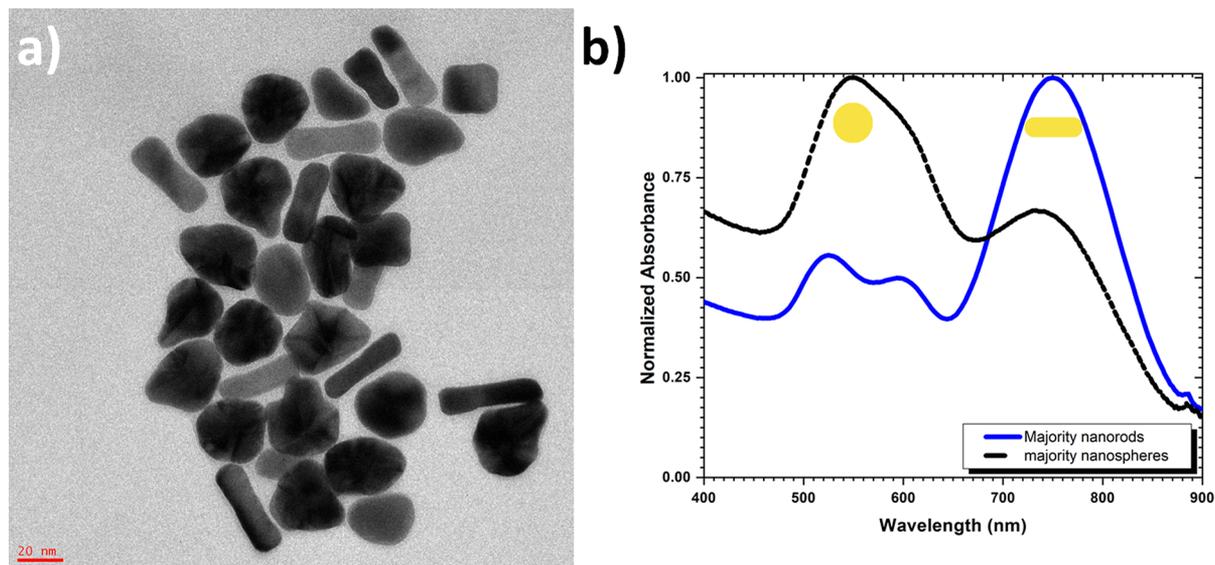

Figure 3. (a) TEM image showing the population of nanorods and nanospheres within the colloidal solution. (b) UV−visible spectra of the nanorods and nanospheres obtained after centrifugation. The black curve displays a majority of nanospheres within the colloidal solution, while the blue curve shows more nanorods within the colloidal solution. The colloidal solution was centrifuged in an attempt to separate the two populations present in the colloidal solution.

(a) The first step lasted for 70 min at approximately 4500 rpm, sufficient to separate the excess amount of CTAB from the surface of nanoparticles. Removal of CTAB was critical to further use of the rods in optoelectronics and biomedical applications.

(b) The second step lasted for ∼20 min at approximately 4500 rpm to separate rods from the spheres in the solution. This method's effectiveness stems from the fact that anisotropic and isotropic particles exhibit different sedimentation speeds, rods segregating in the solution's upper region. In contrast, the spheres settle down at the bottom. Figure 3a,b shows the distribution of nanoparticles and the normalized absorption spectra of the colloidal solution after the two-step centrifugation process, respectively. A comprehensive percentage contribution of rods and particle size distribution are

provided in the Supporting Information. In Figure 3b, the black curve reveals that most particles are spheres as the surface transverse plasmon resonance peak appearing around ∼525 nm dominates over the longitudinal plasmon resonance at ∼750 nm. Similarly, the blue curve suggests that the colloidal solution consists of rods as the LSPR peak dominates the TSPR peak. The intersection of blue and red curves occurring at ∼700 nm corresponds to a critical wavelength in the nanorod formation. At this stage, instead of growing symmetrically in three-dimension, the nanoparticles favor a unidimensional growth while keeping the two other dimensions more or less unchanged.

2.5. Characterization of Nanorods by Transmission Electron Microscopy. Transmission electron microscopy (TEM) was performed using a JEOL 2100-F TEM operating at
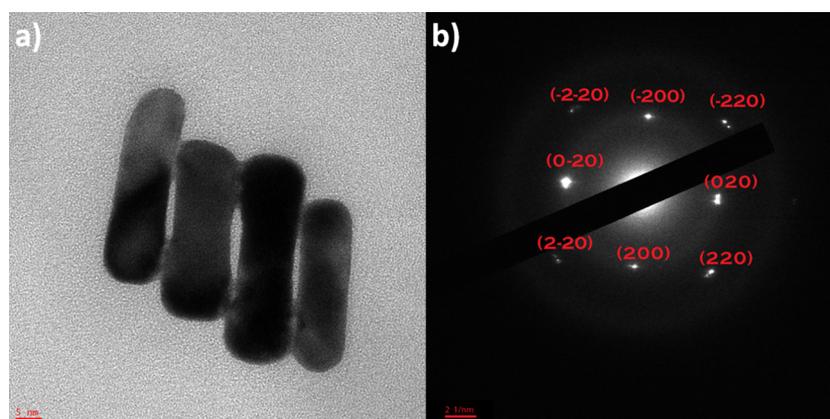
Figure 4. (a) TEM image of nanorods showing the dumbbell-shaped morphology having a length of approximately 40 nm and a width of ~15 nm. (b) Diffraction pattern of dumbbell nanorods showing different planes.

80 kV. In Figure 4a, an image of gold dumbbell nanostructures is displayed. Their length is ~40 nm and the diameter is ~15 nm. Figure 4b shows that the diffraction pattern of the gold dumbbells confirms the cubic crystalline structure of the nanorods. The gold dumbbell nanorods are formed by the {200} and {220} facets.

Let us try to understand the growth of gold dumbbell nanorods. During the wet-chemical synthesis, two types of surface cappings were used: CTAB and $AgNO_3$. Those agents selectively bind to certain facets of the growing gold nanoparticle by reducing the surface energy of those facets relatively to others.[17] By looking at Table 1, the {111} family

Table 1. Surface Energies of Gold and Surfactants Used during the Synthesis

surface energy	Au	CTAB	$AgNO_3$
experimental value (J/m^2)	1.500^{19}	0.040^{20}	0.060^{21}
theoretical value for a (111) facet (J/m^2)	1.283^{19}		
theoretical value for a (100) facet (J/m^2)	1.627^{19}		
theoretical value for a (110) facet (J/m^2)	1.700^{19}		

of planes is found to be less energetic compared to those of families {100} and {110}. Therefore, without surfactants, facets belonging to the {111} family, such as the (222) facets, would grow isometrically to form a spherical or "near-spherical" morphology. However, the situation is different with surfactants because the adhesion of the surfactants to the nanoparticle's surface changes the surface energy of those facets drastically. Indeed, CTAB attached preferentially to {100} facets rather than to {111}; therefore, CTAB allows the growth of more energetic facets as {100}. Consequently, it seems that the high surface energy facets such as (200), belonging to the {100} family, are protected by being covered by CTAB surfactants. While the low surface energy facets (222) do not survive the synthesis conditions, the (222) facets do not appear in the diffraction pattern. The other surfactant used in the synthesis is $AgNO_3$. Grzelczak et al.[18] showed that silver ions attached preferentially according to the following sequence: first on {110}, then on {100}, and lastly on {111}. The silver ions attaching to the {110} facets have five neighboring gold atoms, while on the {111} and {100} surfaces, adsorbed silver ions have just three and four neighbors, respectively. Having more neighbors stabilizes the {110} family of planes, consequently explaining the apparition
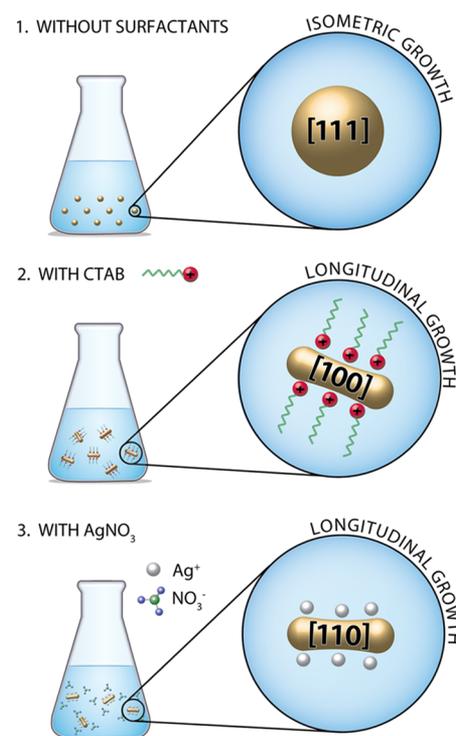
of (220) in the diffraction pattern (Figure 4b). The growth rate of {100} and {110} is therefore controlled by CTAB and $AgNO_3$, respectively. This selectivity gives us control over the aspect ratio of the nanorods.

The role of each surfactant in GND formation is summarized in Figure 5.

Figure 5. Effect of surfactants on the growth of GNDs. (1) In the absence of surfactants, the growth favors the isotropic direction {111} resulting in nanospheres. (2) In the presence of CTAB, anisotropic growth occurs through the energetic facet {100}. (3) In the presence of $AgNO_3$, it favors {110} in the longitudinal direction.

2.6. Characterization of Dumbbell Nanorods Using DLS. Dynamic light scattering (DLS) was performed using a NanoBrook 90Plus Zeta from Brookhaven Instruments Corporation (Figure 6). The first peak in each spectra corresponds to the diameter, while the second peak corresponds to the length of the dumbbell nanorod. The
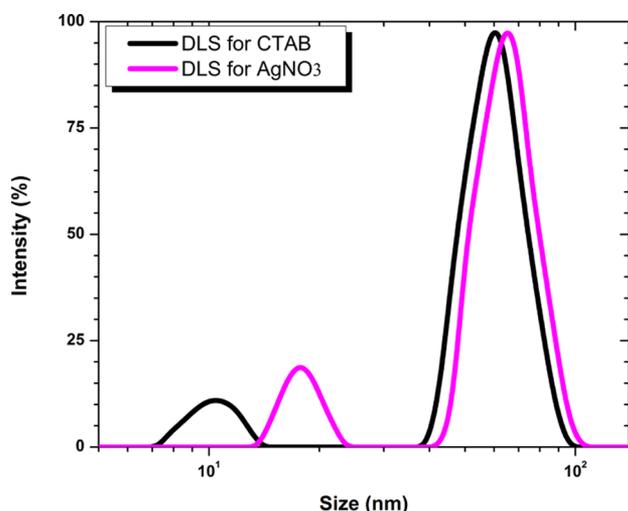
Figure 6. Typical DLS spectra showing two peaks corresponding to the diameter of the rod and the length of the rod.

smaller diameter dumbbell nanorod structures seems to be obtained with CTAB than with AgNO$_3$. Regarding the length,

it seems that either CTAB or AgNO$_3$ gives more or less the same length. The length and diameter measured by DLS are in relatively good agreement with the TEM observations (Figure 4).

From Figure 7a,b, the volumes of CTAB and of AgNO$_3$ seem to evolve linearly with the length of the GND. The control on the nanorod morphology can be explained using the surface-to-volume ratio of rods, as depicted by the analytical model assuming that each GND with two end spheres of diameter D was separated by a middle section cylinder of L whose diameter d is approximated by 90% of D, as illustrated in Figure 7c,d. In Figure 7c, the diameter of end spheres D and the diameter of the middle section d were kept constant, while the length of the middle section was increased which resulted in a decreasing trend of surface-to-volume ratio. Similarly, when the length as well as the diameter of the middle section of the rod were fixed, a significant increase in the surface-to-volume ratio was noticed (Figure 7d).

3. DISCUSSION

In this study, we synthesized the GNDs and characterized them quantitatively. It could be observed that AgNO$_3$ is far
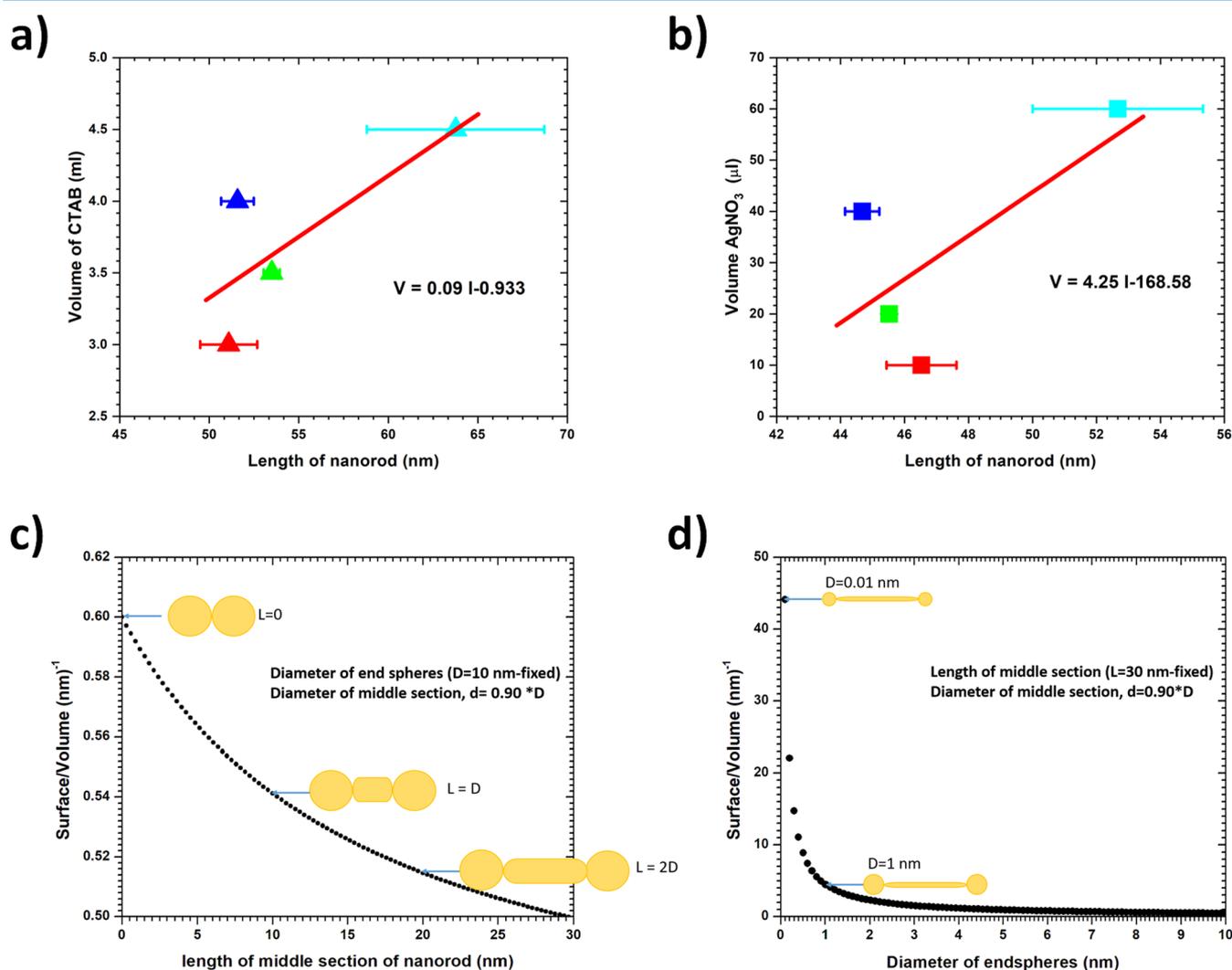

Figure 7. Effect of variation of (a) CTAB and (b) AgNO$_3$ over the length of nanorods. Schematic showing the consequence of change in the (c) length and (d) diameter of dumbbells on the surface-to-volume ratio.
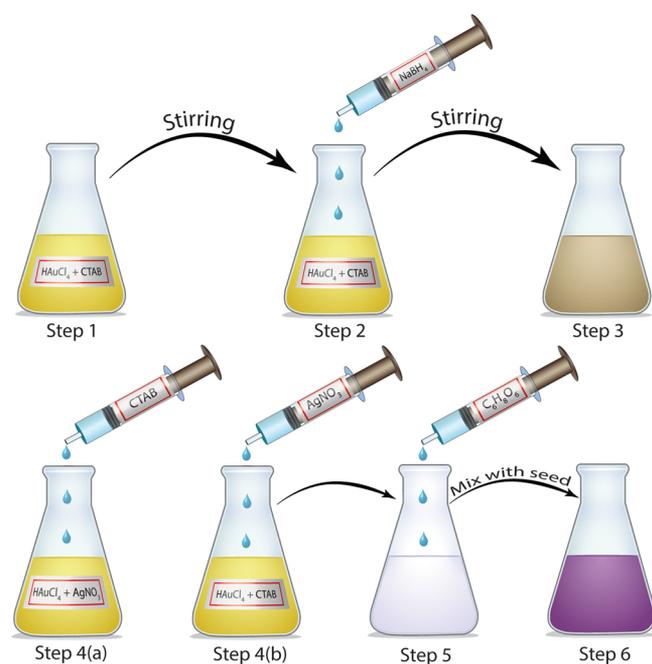
Figure 8. Schematic of a six-step synthesis leading to the growth of GNDs. In steps (1−3), we prepared tiny gold seeds (light brown color) by reducing gold salts by CTAB in the presence of NaBH₄. In step 4a, we added CTAB in the stock solution of gold salts and AgNO₃ to study the effect of CTAB concentration on the formation of rods. In step 4b, we studied the effect of silver nitrate, keeping the gold salts and CTAB constant using seeds from the first stage. In step 5, ascorbic acid was dropped into the solution obtained from steps 4a and 4b to obtain the final product as dumbbell-shaped nanoparticles (purple/violet) (step 6).

more influential than CTAB in controlling the aspect ratio. The aspect ratio increases linearly with CTAB and AgNO₃ within the investigated range. A dumbbell with an aspect ratio of 3.5 requires about 3.5 mL of CTAB with no AgNO₃, whereas only 35 μL of AgNO₃ could produce the same aspect ratio of 3.5 without CTAB. If GNDs are approximated as tiny cylinders with two end spheres, then for a fixed length, the surface area-to-volume ratio is pronounced for diameters less than 1 nm. This observation translates into the fact that GNDs with optimized morphology can be excellent drug carriers in therapeutic medical treatments.

As the length of GNDs increased, the UV spectra moved right. Other researchers who investigated GNRs have made similar observations; however, the shift also depended upon the chemicals and their concentration. Thambi *et al.* investigated the formation of different-shaped GNRs by varying the pH of the original growth solution.[22] The spectra started shifting left as the pH increased due to the formation of different endcaps. Xu *et al.* used a gemini surfactant to replace CTAB in the growth solution and investigated the effect of the gemini surfactant (P16-8-16) on the shape of GNRs.[23] As the surfactant concentration varied from 12 to 24 mM, the longitudinal extinction spectrum peak shifted left, while the transverse peak shifted slightly to the right indicating a change in morphology.

Gou and Murphy suggested that CTAB had preferential affinity along the longitudinal surface of nanorods by coating the surface while exposing the ends to gold ions resulting in non-uniform GNRs (i.e. dog-bone-shaped).[24] We believe that

we could agree with their suggestion based on the growth mechanism presented earlier in this paper.

The morphology of GNRs appears to be dependent upon the concentration of chemicals used, pH, and the amount of seed solution. We observed that the concentration of CTAB and AgNO₃ controls the morphology of GNDs. Shi *et al.* examined the effect of seed amount, ascorbic acid amount, and AgNO₃ amount on the growth of the nanorods.[14] They found that increasing the amount of seed solution reduced the length of the nanorods. This finding was compatible with a similar conclusion from Xu *et al.*[23] Also, by controlling the pH of the seed, the length of nanorods can be tuned. In particular, the low pH value of the seed favors the elongation of the rods by stabilizing the CTAB micelles and hindering the reducing behavior of ascorbic acid.[25] Our observation is compatible with the observation of Shi *et al.*[14] who concluded that the silver ion concentration and the seed/Au³⁺ ratio were most effective in controlling the morphology. The concentration of ascorbic acid was also found to be affecting the morphology. Saute and Narayana, while examining the SERS effect on thiram,[12] used a slightly modified seed-mediated growth method reported by Gou and Murphy,[24] Murphy *et al.*,[10] and Sau and Murphy[26] and controlled the size of nanoparticles by changing the concentration of ascorbic acid in the growth solution. Recently, a few works have published the alternatives for ascorbic acid such as hydroquinone,[27] dopamine,[28] and 3-aminophenol[29] to increase the monodispersity and the conversion ratio of gold ions to GNRs.

Interestingly, only a few studies have been performed on GNDs. The UV spectrum shift has been observed in those studies as well. Huang *et al.*[30] synthesized GNDs using an electrochemical method. Their results showed that the UV spectra shifted right when GNRs transitioned from spheres to long rods through the phases of short rods and dumbbells. Stender *et al.* examined the plasmonic behavior of gold GNDs both experimentally and theoretically.[31] They simulated GNDs with different lobe sizes and shapes. The dumbbell with rounded lobes showed a greater red shift in the longitudinal plasmon resonance peak (LSPR) than with angular lobes. Park *et al.* electrochemically synthesized the Au−Ni−Au dumbbell by employing a seed-mediated growth strategy to deposit Au atoms onto Au−Ni−Au nanorods.[32] They also observed that the LSPR of dumbbells red-shifted compared to the LSPR of nanorods. Here, in this work, by varying two surfactants, we were able to tune the LSPR to ∼669−789 nm. Since the adjusted spectral range is beyond 700 nm, the GNDs could be a potential candidate for photothermal applications. In order to use nanoparticles as photothermal agents, the particle needs to absorb 700−2500 nm,[33] which is often referred to as biological windows, namely, I-BW (700−980 nm) and II-BW (1000−1400 nm), corresponding to minimum light absorption by hemoglobin and water.[34]

In Table 2, we summarize the GNR and GND synthesis protocols reported in the literature. Such a summary will help researchers quickly obtain critical information on previous work.

4. CONCLUSIONS

In this work, we demonstrated the growth of dumbbell-shaped nanorods by varying the concentration of CTAB and AgNO₃ using the seed method. Our results suggest that the employed method can easily modify the shape, size, and overall aspect ratio of the dumbbell nanostructures. Also, this method

Table 2. Summary of Synthesis Protocol Related to GNRs of Different Forms and GNDs

published year	reagents in growth solution	concentration	synthesis protocol	varied parameters	λ_{max} (nm)
				Longitudinal Nanorods of Different Shapes	
ACS Omega (2019)[22]	AA	0.0788 M	SMG + HCl (11.3 M) in growth solution + overgrowth	NRs were obtained first and then subjected to pH variation. pH values of 8 (w/o Ag) and 4 (with Ag) resulted in dog-bone-shaped NRs	577–777
	CTAB + $C_{18}H_{33}NaO_2$	0.2 M			
	AgNO$_3$	40 mM			
	AA	64 mM			
Mat. Res. Express (2019)[35]	HAuCl$_4$	0.1 M	SMG + HCl (0.2 M) in growth solution		a
	CTAB	0.1 M			
	AgNO$_3$	0.01 M			
	AA	0.1 M			
Nanoscale (2015)[23]	HAuCl$_4$	0.25 mM	SMG + HCl (10 mM)) in growth solution	variation of conc. of the gemini surfactant from 12 to 24 mM resulted in straight NRs to curved dog-bone-shaped bones	660–960
	gemini surfactant	12 Mm			
	AgNO$_3$	0.3 mM			
	AA	0.32 mM			
ISRN Nanomater. (2012)[14]	HAuCl$_4$	1 mM	SMG	concentration of AA greater than 0.1 M resulted in dog-bone-shaped NRs	600–1050
	CTAB	0.2 M			
	AgNO$_3$	4 mM			
	AA	0.1 M			
Analyst (2011)[12]	HAuCl$_4$	0.01 M	SMG	AA was varied from 0.1 to 0.25 M to get larger dog-bone-shaped NRs	671–758
	CTAB	0.1 M			
	AgNO$_3$	0.01 M			
	AA	0.1 M			
J. Cryst. Growth (2009)[36]	HAuCl$_4$	0.25 mM	SMG	especially the single crystalline seed size of 1.5 nm resulted in dog-bone-shaped NRs	a
	CTAB	100 mM			
	AgNO$_3$	50 μm			
	AA	0.1 M			
Adv. Funct. Mater. (2006)[11]	HAuCl$_4$	0.5 mM	SMG		a
	CTAB	0.2 M			
	AgNO$_3$	0–0.25 mM			
	AA	a			
Nanotechnology (2007)[37]	HAuCl$_4$	0.01 M	SMG	different amounts of AA were introduced into the solution to grow dog-bone-shaped NRs	676–713
	CTAB	0.10 M			
	AgNO$_3$	0.01 M			
	AA	0.1 M			
Nanotechnology (2005)[38]	HAuCl$_4$	0.01 M	SMG	pH was varied from 3.6 to 9.6 to obtain dog-bone-shaped NRs	605–729
	CTAB	0.1 M			
	AgNO$_3$	4 mM			

Table 2. continued

published year	reagents in growth solution	concentration	synthesis protocol	varied parameters	λ_{max} (nm)
				Longitudinal Nanorods of Different Shapes	
Chem. Mater. (2005)[24]	AA HAuCl$_4$ CTAB AgNO$_3$ AA	0.1 M 0.1 M 0.1 M 0.01 M 1.1 M	SMG	different amounts of AA were added to the growth solution for dog-bone-shaped particles	a
				Gold Dumbbell Nanorods	
JCIS (2006)[30]	CTAB TTABr	0.08 M a	electrochemical method	current 5 mA, electrolysis carried out for 20 min at 360 C in the presence of acetone to get a single crystalline dumbbell	690–880
Langmuir (2004)[39]	silver ions AA glycine buffer	0.097 mM 0.53 mM 500 mM	SMG	pH was varied from 8 to 10 to obtain bimetallic dumbbell-shaped Au–Ag core–shell NRs	637–797
JPCC (2013)[31]	acquired from Nanopartz, Inc	a	a	a	a
JECST (2012)[32]	HAuCl$_4$ CTAB NaOH AA	0.05 M 0.05 mM 5 μM 5–12.5 μM	SMG and electrochemical deposition	Au–Ni–Au triblock NRs were made by the AAO template and electrochemical deposition Further selective growth of Au on the Au surface via solution-phase chemical growth resulted in dumbbell-like NRs.	>1600
J. Mater. Chem. (2012)[40]	HAuCl$_4$ CTAB AgNO$_3$ BDAC	5 × 10^{-4} M 0.20 M 0.004 M 0.15 M	SMG	(a) 0.1 M NaOH on NR seed in the growth solution to get spherical-ended dumbbells (b) different amounts of AA were introduced into the seed to obtain arrow-ended dumbbell-shaped NRs	802–930 (spherical ended) 884–996 (arrow ended)
Adv. Mater. (2001)[41]	HAuCl$_4$ CTAB AgNO$_3$ AA	250 μM 0.20 M 10 mM 10 mM	SMG	addition of 10 mM AgNO$_3$ with 10 mM AA resulted in the growth of spheroids and rods	600–1600
our method	HAuCl$_4$ CTAB AgNO$_3$ AA	0.01 M 0.1 M 0.01 M 0.1 M	SMG	concentrations of CTAB and AgNO$_3$ are varied separately keeping other parameters constant and leaving the solution undisturbed for 4–5 days to let it grow fully	669–789

^{a}Not provided.

provides a simple way to tune LSPR within 120 nm suggesting that there exists a critical wavelength where the growth of nanoparticles hinders the movement in the symmetric direction forcing the particle to move forward unidirectionally. We also demonstrated that the DLS was a valuable complimentary characterization when backed up with TEM observations.

5. EXPERIMENTAL SECTION

5.1. Materials and Reagents. All the chemicals required for the chemical synthesis of nanorods were purchased from Sigma-Aldrich and were used as received. These include gold acid chloride trihydrate (HAuCl$_4$. 3H$_2$O, 99.9%), silver nitrate (AgNO$_3$ 99.9999%), L-ascorbic acid (C$_6$H$_8$O$_6$, 99.5%), CTAB (99.9%), and sodium borohydride (NaBH$_4$, 99.99%). Deionized (DI) water was used to prepare the colloidal solutions and clean glassware was used to avert the outside contaminants.

5.2. Chemical Synthesis of Nanoparticles. Au-NRs were prepared by employing a SMG.[41] Steps 1−3 demonstrate the seed preparation, where 0.010 M gold salts (HAuCl$_4$) and 0.100 M CTAB were stirred for 10 min. Then, 0.010 M NaBH$_4$ prepared in ice-cold DI water was added dropwise and stirred for another 10 min at a higher speed to obtain a transparent light brown solution of the seed. In step 4a, distinct concentrations of CTAB were first mixed with 0.010 M HAuCl$_4$ and 0.010 M AgNO$_3$, followed by the addition of 0.100 M L-ascorbic acid to obtain a colorless solution. The seed solution was then added and gently mixed by inversion for several seconds, generating a dark violet solution, under a minute. The samples were then placed in a water bath around 34 °C for approximately 4 days, allowing the rods to grow. In step 4b, we repeated step 4a by varying the concentration of AgNO$_3$ while maintaining the stock solution of 0.010 M HAuCl$_4$ and 0.010 M CTAB.

5.3. Material Characterization. A Shimadzu UV 2450 PC spectrometer obtained the colloidal solution's UV−visible absorption spectra by comparing the monochromatic beam attenuation as it passes through a 1 cm quartz cuvette of the sample versus the precursor. TEM was performed at 80 kV using a JEOL 2100-F to obtain the size, morphology, and crystal structure. DLS was performed with a NanoBrook 90Plus Zeta from Brookhaven Instruments Corporation.

ASSOCIATED CONTENT

ⓈI Supporting Information

The Supporting Information is available free of charge at https://pubs.acs.org/doi/10.1021/acsomega.0c06062.

> Summary of nanoparticles' dimensions obtained at−various CTAB concentrations keeping the AgNO$_3$ concentration constant and of those obtained at various AgNO$_3$ concentrations keeping the CTAB concentration constant; quantitative analysis of dumbbell-shaped nanorods and nanospheres performed by varying the CTAB concentration and keeping the AgNO$_3$ concentration constant and by varying the AgNO$_3$ concentration and keeping the CTAB concentration constant (PDF)

AUTHOR INFORMATION

Corresponding Author

Puskar Chapagain − *Department of Engineering and Physics, Southern Arkansas University, Magnolia, Arkansas 71753, United States;* ⓞ orcid.org/0000-0002-0906-5711; Email: prchapagain@saumag.edu

Authors

Grégory Guisbiers − *Department of Physics and Astronomy, University of Arkansas at Little Rock, Little Rock, Arkansas 72204, United States;* ⓞ orcid.org/0000-0002-4615-6014

Matthew Kusper − *Department of Physics and Astronomy, University of Arkansas at Little Rock, Little Rock, Arkansas 72204, United States;* ⓞ orcid.org/0000-0002-9239-6262

Luke D. Geoffrion − *Department of Physics and Astronomy, University of Arkansas at Little Rock, Little Rock, Arkansas 72204, United States;* ⓞ orcid.org/0000-0003-4668-7453

Mourad Benamara − *Department of Microelectronics and Photonics, University of Arkansas, Fayetteville, Arkansas 72701, United States*

Alexander Golden − *Department of Engineering and Physics, Southern Arkansas University, Magnolia, Arkansas 71753, United States; Department of Microelectronics and Photonics, University of Arkansas, Fayetteville, Arkansas 72701, United States*

Abdel Bachri − *Department of Engineering and Physics, Southern Arkansas University, Magnolia, Arkansas 71753, United States*

Lionel Hewavitharana − *Department of Engineering and Physics, Southern Arkansas University, Magnolia, Arkansas 71753, United States;* ⓞ orcid.org/0000-0001-9049-6836

Complete contact information is available at:
https://pubs.acs.org/10.1021/acsomega.0c06062

Notes

The authors declare no competing financial interest.

REFERENCES

(1) Guisbiers, G.; Mendoza-Cruz, R.; Bazán-Díaz, L.; Velázquez-Salazar, J. J.; Mendoza-Perez, R.; Robledo-Torres, J. A.; Rodriguez-Lopez, J.-L.; Montejano-Carrizales, J. M.; Whetten, R. L.; José-Yacamán, M. Electrum, the Gold−Silver Alloy, from the Bulk Scale to the Nanoscale: Synthesis, Properties, and Segregation Rules. *ACS Nano* **2016**, *10*, 188−198.

(2) Guisbiers, G.; Mejia-Rosales, S.; Khanal, S.; Ruiz-Zepeda, F.; Whetten, R. L.; José-Yacaman, M. Gold−Copper Nano-Alloy,

"Tumbaga", in the Era of Nano: Phase Diagram and Segregation. *Nano Lett.* **2014**, *14*, 6718−6726.

(3) Yu, Y.-Y.; Chang, S.-S.; Lee, C.-L.; Wang, C. R. C. Gold Nanorods: Electrochemical Synthesis and Optical Properties. *J. Phys. Chem. B* **1997**, *101*, 6661−6664.

(4) Daniel, M.-C.; Astruc, D. Gold Nanoparticles: Assembly, Supramolecular Chemistry, Quantum-Size-Related Properties, and Applications toward Biology, Catalysis, and Nanotechnology. *Chem. Rev.* **2004**, *104*, 293−346.

(5) Nikoobakht, B.; El-Sayed, M. A. Surface-Enhanced Raman Scattering Studies on Aggregated Gold Nanorods. *J. Phys. Chem. A* **2003**, *107*, 3372−3378.

(6) Obare, S. O.; Jana, N. R.; Murphy, C. J. Preparation of Polystyrene- and Silica-Coated Gold Nanorods and Their Use as Templates for the Synthesis of Hollow Nanotubes. *Nano Lett.* **2001**, *1*, 601−603.

(7) Liu, M.; Guyot-Sionnest, P. Synthesis and Optical Characterization of Au/Ag Core/Shell Nanorods. *J. Phys. Chem. B* **2004**, *108*, 5882−5888.

(8) Foss, C. A., Jr.; Hornyak, G. L.; Stockert, J. A.; Martin, C. R. Optical Properties of Composite Membranes Containing Arrays of Nanoscopic Gold Cylinders. *J. Phys. Chem.* **1992**, *96*, 7497−7499.

(9) Chang, S.-S.; Shih, C.-W.; Chen, C.-D.; Lai, W.-C.; Wang, C. R. C. The Shape Transition of Gold Nanorods. *Langmuir* **1999**, *15*, 701−709.

(10) Murphy, C. J.; Sau, T. K.; Gole, A. M.; Orendorff, C. J.; Gao, J.; Gou, L.; Hunyadi, S. E.; Li, T. *Anisotropic Metal Nanoparticles: Synthesis, Assembly, and Optical Applications*; ACS Publications, 2005.

(11) Xu, X.; Cortie, M. B. Shape Change and Color Gamut in Gold Nanorods, Dumbbells, and Dog Bones. *Adv. Funct. Mater.* **2006**, *16*, 2170−2176.

(12) Saute, B.; Narayanan, R. Solution-Based Direct Readout Surface Enhanced Raman Spectroscopic (SERS) Detection of Ultra-Low Levels of Thiram with Dogbone Shaped Gold Nanoparticles. *Analyst* **2011**, *136*, 527−532.

(13) Chen, H.; Shao, L.; Li, Q.; Wang, J. Gold Nanorods and Their Plasmonic Properties. *Chem. Soc. Rev.* **2013**, *42*, 2679−2724.

(14) Shi, W.; Casas, J.; Venkataramasubramani, M.; Tang, L. Synthesis and Characterization of Gold Nanoparticles with Plasmon Absorbance Wavelength Tunable from Visible to near Infrared Region. *ISRN Nanomater.* **2012**, *2012*, 659043.

(15) Demeler, B.; Nguyen, T.-L.; Gorbet, G. E.; Schirf, V.; Brookes, E. H.; Mulvaney, P.; El-Ballouli, A. a. O.; Pan, J.; Bakr, O. M.; Demeler, A. K.; Hernandez Uribe, B. I.; Bhattarai, N.; Whetten, R. L. Characterization of Size, Anisotropy, and Density Heterogeneity of Nanoparticles by Sedimentation Velocity. *Anal. Chem.* **2014**, *86*, 7688−7695.

(16) Scaletti, F.; Kim, C. S.; Messori, L.; Rotello, V. M. Rapid Purification of Gold Nanorods for Biomedical Applications. *Methodsx* **2014**, *1*, 118−123.

(17) Guisbiers, G.; José-Yacaman, M. Use of Chemical Functionalities to Control Stability of Nanoparticles. In *Encyclopedia of Interfacial Chemistry*; Wandelt, K., Ed.; Elsevier: Oxford, 2018; pp 875−885.

(18) Grzelczak, M.; Pérez-Juste, J.; Mulvaney, P.; Liz-Marzán, L. M. Shape Control in Gold Nanoparticle Synthesis. *Chem. Soc. Rev.* **2008**, *37*, 1783.

(19) Vitos, L.; Ruban, A. V.; Skriver, H. L.; Kollár, J. The Surface Energy of Metals. *Surf. Sci.* **1998**, *411*, 186−202.

(20) Shah, S. K.; Bhattarai, A. Interfacial and Micellization Behavior of Cetyltrimethylammonium Bromide (CTAB) in Water and Methanol-Water Mixture at 298.15 to 323.15 K. https://www.hindawi.com/journals/jchem/2020/4653092/ (accessed Nov 13, 2020).

(21) Kamali, M. J.; Kamali, Z.; Vatankhah, G. Thermodynamic Modeling of Surface Tension of Aqueous Electrolyte Solution by Competitive Adsorption Model. https://www.hindawi.com/journals/jther/2015/319704/ (accessed Nov 13, 2020).

(22) Thambi, V.; Kar, A.; Ghosh, P.; Paital, D.; Gautam, A. R. S.; Khatua, S. Synthesis of Complex Nanoparticle Geometries via PH-Controlled Overgrowth of Gold Nanorods. *ACS Omega* **2019**, *4*, 13733−13739.

(23) Xu, Y.; Zhao, Y.; Chen, L.; Wang, X.; Sun, J.; Wu, H.; Bao, F.; Fan, J.; Zhang, Q. Large-Scale, Low-Cost Synthesis of Monodispersed Gold Nanorods Using a Gemini Surfactant. *Nanoscale* **2015**, *7*, 6790−6797.

(24) Gou, L.; Murphy, C. J. Fine-Tuning the Shape of Gold Nanorods. *Chem. Mater.* **2005**, *17*, 3668−3672.

(25) Ni, W.; Kou, X.; Yang, Z.; Wang, J. Tailoring Longitudinal Surface Plasmon Wavelengths, Scattering and Absorption Cross Sections of Gold Nanorods. *ACS Nano* **2008**, *2*, 677−686.

(26) Sau, T. K.; Murphy, C. J. Room Temperature, High-Yield Synthesis of Multiple Shapes of Gold Nanoparticles in Aqueous Solution. *J. Am. Chem. Soc.* **2004**, *126*, 8648−8649.

(27) Chang, H.-H.; Murphy, C. J. Mini Gold Nanorods with Tunable Plasmonic Peaks beyond 1000 Nm. *Chem. Mater.* **2018**, *30*, 1427−1435.

(28) Su, G.; Yang, C.; Zhu, J.-J. Fabrication of Gold Nanorods with Tunable Longitudinal Surface Plasmon Resonance Peaks by Reductive Dopamine. *Langmuir* **2015**, *31*, 817−823.

(29) Wu, Z.; Liang, Y.; Cao, L.; Guo, Q.; Jiang, S.; Mao, F.; Sheng, J.; Xiao, Q. High-Yield Synthesis of Monodisperse Gold Nanorods with a Tunable Plasmon Wavelength Using 3-Aminophenol as the Reducing Agent. *Nanoscale* **2019**, *11*, 22890−22898.

(30) Huang, C.-J.; Chiu, P.-H.; Wang, Y.-H.; Yang, C.-F. Synthesis of the Gold Nanodumbbells by Electrochemical Method. *J. Colloid Interface Sci.* **2006**, *303*, 430−436.

(31) Stender, A. S.; Wei, X.; Augspurger, A. E.; Fang, N. Plasmonic Behavior of Single Gold Dumbbells and Simple Dumbbell Geometries. *J. Phys. Chem. C* **2013**, *117*, 16195−16202.

(32) Park, Y. J.; Liu, L.; Yoo, S.-H.; Park, S. Electrochemical Synthesis of Dumbbell-like Au-Ni-Au Nanorods and Their Surface Plasmon Resonance. *J. Electrochem. Sci. Technol.* **2012**, *3*, 57−62.

(33) Jaque, D.; Martínez Maestro, L.; del Rosal, B.; Haro-Gonzalez, P.; Benayas, A.; Plaza, J. L.; Martín Rodríguez, E.; García Solé, J. Nanoparticles for Photothermal Therapies. *Nanoscale* **2014**, *6*, 9494−9530.

(34) Bazán-Díaz, L.; Mendoza-Cruz, R.; Velázquez-Salazar, J. J.; Plascencia-Villa, G.; Romeu, D.; Reyes-Gasga, J.; Herrera-Becerra, R.; José-Yacamán, M.; Guisbiers, G. Gold−Copper Nanostars as Photo-Thermal Agents: Synthesis and Advanced Electron Microscopy Characterization. *Nanoscale* **2015**, *7*, 20734−20742.

(35) Ahmad, I.; Khan, H. U.; Jan, R.; Khan, S. A. Anisotropic Gold Nanoparticles Crystalizes in Multifaceted Superstructures. *Mater. Res. Express* **2019**, *6*, 105006.

(36) Kawamura, G.; Nogami, M. Application of a Conproportionation Reaction to a Synthesis of Shape-Controlled Gold Nanoparticles. *J. Cryst. Growth* **2009**, *311*, 4462−4466.

(37) Huang, C.-J.; Chiu, P.-H.; Wang, Y.-H.; Meen, T.-H.; Yang, C.-F. Synthesis and Characterization of Gold Nanodogbones by the Seeded Mediated Growth Method. *Nanotechnology* **2007**, *18*, 395603.

(38) Wang, C.; Wang, T.; Ma, Z.; Su, Z. PH-Tuned Synthesis of Gold Nanostructures from Gold Nanorods with Different Aspect Ratios. *Nanotechnology* **2005**, *16*, 2555−2560.

(39) Huang, C.-C.; Yang, Z.; Chang, H.-T. Synthesis of Dumbbell-Shaped Au- Ag Core- Shell Nanorods by Seed-Mediated Growth under Alkaline Conditions. *Langmuir* **2004**, *20*, 6089−6092.

(40) Wang, P.; Liu, M.; Gao, G.; Zhang, S.; Shi, H.; Li, Z.; Zhang, L.; Fang, Y. From Gold Nanorods to Nanodumbbells: A Different Way to Tailor Surface Plasmon Resonances by a Chemical Route. *J. Mater. Chem.* **2012**, *22*, 24006−24011.

(41) Jana, N. R.; Gearheart, L.; Murphy, C. J. Seed-Mediated Growth Approach for Shape-Controlled Synthesis of Spheroidal and Rod-like Gold Nanoparticles Using a Surfactant Template. *Adv. Mater.* **2001**, *13*, 1389−1393.